

## Resonant photon absorption and hole burning in Cr<sub>7</sub>Ni antiferromagnetic rings

W. Wernsdorfer,<sup>1</sup> D. Mailly,<sup>2</sup> G. A. Timco,<sup>3</sup> and R. E. P. Winpenny<sup>3</sup>

<sup>1</sup>Laboratoire Louis Néel, associé à l'UJF, CNRS, BP 166, 38042 Grenoble Cedex 9, France

<sup>2</sup>LPN, CNRS, Route de Nozay, 91460 Marcoussis, France

<sup>3</sup>Department of Chemistry, The University of Manchester, Oxford Road, Manchester M13 9PL, UK

(Received 27 June 2005; published 29 August 2005)

Magnetization measurements on a crystal of Cr<sub>7</sub>Ni antiferromagnetic rings are presented. Irradiation with microwaves at frequencies between 1 and 10 GHz leads to observation of very narrow Gaussian resonant photon absorption lines which are mainly broadened by hyperfine interactions. The relaxation of magnetization after a nanosecond RF pulse is dominated by the phonon bottleneck effect. A two-pulse hole burning technique allowed us to estimate the characteristic energy diffusion time (spectral diffusion).

DOI: 10.1103/PhysRevB.72.060409

PACS number(s): 75.50.Xx, 75.60.Jk, 75.75.+a, 76.30.-v

Magnetic molecules are currently considered among the most promising electron spin based quantum systems for the storing and processing of quantum information.<sup>1</sup> For this purpose, ferromagnetic<sup>2</sup> and antiferromagnetic<sup>3,4</sup> systems have attracted an increasing interest.<sup>5,6</sup> In the latter case the quantum hardware is thought of as a collection of coupled molecules, each corresponding to a different qubit. The main advantages would arise from the fact that they are extremely small and almost identical, allowing to obtain, in a single measurement, statistical averages of a large number of qubits. The magnetic properties can be modeled with an outstanding degree of accuracy. And most importantly, the desired physical properties can be engineered chemically.

Recently, the suitability of Cr-based antiferromagnetic molecular rings for the qubit implementation has been proposed.<sup>5,6</sup> The substitution of one metal ion in a Cr-based molecular ring with dominant antiferromagnetic couplings allows its level structure and ground-state degeneracy to be engineered.<sup>7,8</sup> A Cr<sub>7</sub>Ni molecular ring was characterized by means of low-temperature specific-heat and torque-magnetometry measurements, thus determining the microscopic parameters of the corresponding spin Hamiltonian. The energy spectrum and the suppression of the leakage-inducing S-mixing render the Cr<sub>7</sub>Ni molecule a suitable candidate for the qubit implementation.<sup>5,6,9</sup>

In this Rapid Communication we report the micro-superconducting quantum interference device (micro-SQUID)<sup>10</sup> studies of the Cr<sub>7</sub>Ni molecular ring. Electron paramagnetic resonance (EPR) methods are combined with high-sensitivity magnetization measurements. The magnetization detection could also be a Hall-probe magnetometer,<sup>11-15</sup> a standard SQUID,<sup>16</sup> or a vibrating sample magnetometer.<sup>17</sup> We found very narrow resonant photon absorption lines which are mainly broadened by hyperfine interactions. A two-pulse hole burning technique allowed us to estimate the characteristic energy diffusion time.

The Cr<sub>7</sub>Ni molecular ring, is based on a homometallic ring with formula [Cr<sub>8</sub>F<sub>8</sub>(O<sub>2</sub>CCMe<sub>3</sub>)<sub>16</sub>]. The eight chromium(III) ions lie at the corners of a regular octagon.<sup>7</sup> Each edge of the octagon is bridged by one fluoride ion and two pivalate ligands. There is a large cavity at the centre of the ring. If a single chromium(III) ion is replaced by a metal(II)

ion, for example nickel(II), this makes the ring anionic and a cation can be incorporated in the cavity. Thus we can make [H<sub>2</sub>NMe<sub>2</sub>][Cr<sub>7</sub>NiF<sub>8</sub>(O<sub>2</sub>CCMe<sub>3</sub>)<sub>16</sub>].<sup>8</sup> If crystallized from a mixture of THF and MeCN the Cr<sub>8</sub> and Cr<sub>7</sub>Ni compounds are isostructural, crystallizing in the tetragonal space group, P4.

The measurements were made in a dilution cryostat using a 20 μm sized single crystal of Cr<sub>7</sub>Ni. The magnetic probe was a micro-SQUID array<sup>10,18</sup> equipped with three coils allowing application of a field in any direction and with sweep rates up to 10 T/s. The electromagnetic radiation was generated by a frequency synthesizer (Anritsu MG3694A) triggered with a nanosecond pulse generator. This setup allows continuous variation of the frequency from 0.1 Hz to 20 GHz, with pulse lengths ~1 ns to continuous radiation.<sup>19</sup> Using a 50 μm sized gold radio frequency (RF) loop, the RF radiation field was directed in a plane perpendicular to the applied static field μ<sub>0</sub>H. The microwave power of the generator could be varied from -80 to 20 dBm (10<sup>-11</sup> to 10<sup>-1</sup> W). The sample absorbs only a small fraction of the generator power. This fraction is however proportional to the microwave power of the generator. The microwave amplitude B<sub>RF</sub> can be estimated with the method described in Ref. 10. We found B<sub>RF</sub> ≈ 1 mT at 4 GHz and 15 dBm which is more than 1000 times larger than in our previous work on V<sub>15</sub>.<sup>10</sup>

Figure 1(a) shows magnetization vs applied field curves for several field sweep rates at a cryostat temperature of 0.04 K. The magnetization loops exhibit a clear hysteresis which is characteristic for the phonon-bottleneck regime with a spin-phonon relaxation time to the cryostat of a few seconds.<sup>20</sup> Note that the degeneracy of the Kramers doublet is lifted due to internal transverse fields (mainly the transverse hyperfine fields). In order to quantify the out-of-equilibrium effect, Fig. 1(b) presents the same data as in Fig. 1(a) but the magnetization *M* is converted into a spin temperature *T<sub>S</sub>* using the equation:<sup>21</sup>

$$M(T_S)/M_S = \tanh(g\mu_B S \mu_0 H / k_B T_S) \quad (1)$$

with *S*=1/2 and *g*=2.1.<sup>8</sup> Figure 1(b) shows clearly a strong adiabatic cooling when sweeping the field down to zero field. Note that this cooling mechanism might be used before qubit

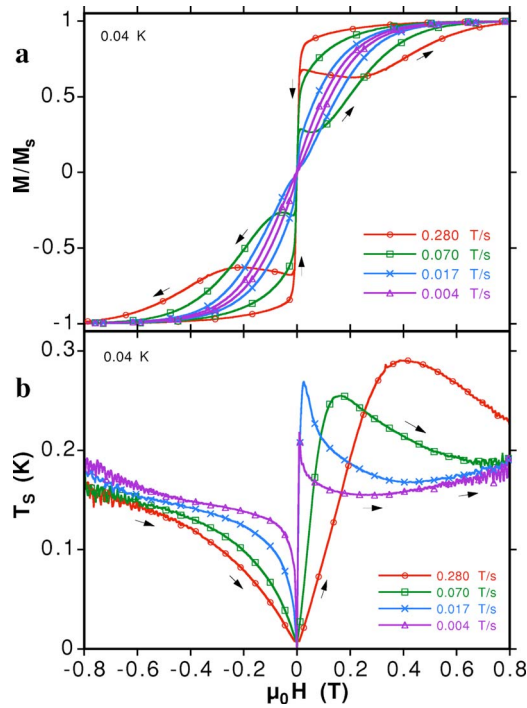


FIG. 1. (Color online) (a) Magnetization ( $M$ ) hysteresis loops for several field sweep rates at a cryostat temperature of 0.04 K. The loops are normalized by the saturation magnetization  $M_s$  at 1.5 T. (b) Spin temperature  $T_s$  for field sweeps from negative to positive fields, obtained by inversion of Eq. (1) where  $M(T_s)$  are the data in (a).

operations to reach extremely low temperatures even at relatively high cryostat temperatures. High frequency noise from the RF-loop around the sample leads to spin temperatures at 1 T being higher than the cryostat temperature.

Figure 2 shows magnetization curves  $M(H)$  in the quasi-static regime with a field sweep rate slow enough

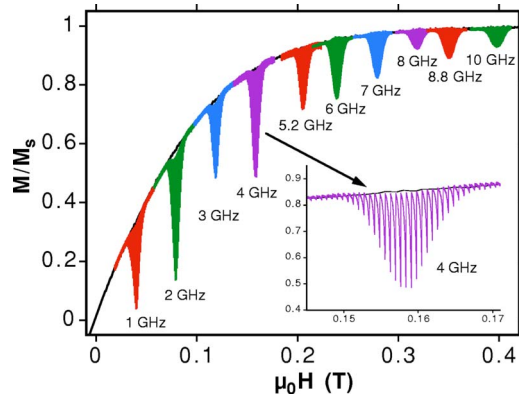


FIG. 2. (Color online) Magnetization curves measured with and without irradiation. The cryostat temperature was 40 mK and the field sweep rate of 0.14 mT/s was slow in order to keep the system at equilibrium. The electromagnetic radiation was pulsed with a period of 4 s and a pulse length of 1  $\mu$ s. The RF frequencies are indicated and the RF amplitude is slightly frequency dependent. Inset: Enlargement of the 4 GHz resonance. The fine structure is due to the RF pulses.

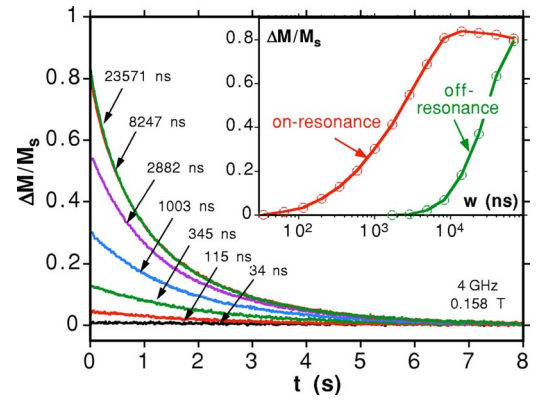


FIG. 3. (Color online) Relaxation of magnetization after a RF pulse of 4 GHz. The pulse lengths  $w$  are indicated. Inset: magnetization variation  $\Delta M$  after a RF pulse vs the pulse length  $w$  for an on-resonance field (0.1582 T) and off-resonance field (0.1722 T).

(0.14 mT/s) to keep the system at equilibrium. During the field sweep, RF pulses were applied to the sample with a pulse length of 1  $\mu$ s and a period of 4 s between each pulse. Depending on the RF frequency, clear dips are observed which result from resonant absorptions of photons associated with spin transitions between the quantum numbers  $m_s = 1/2$  and  $-1/2$ . After each pulse, the magnetization relaxes back to the equilibrium magnetization (see the fine structure in the inset of Fig. 2).

Typical relaxation measurements at a constant applied field after RF pulses of different durations are shown in Fig. 3. The relaxation is exponential with the rate independent of the pulse length. Detailed studies showed that the relaxation rate is dominated by the phonon-bottleneck regime, that is the spin-phonon relaxation time to the cryostat.

The inset of Fig. 3 presents the change of magnetization  $\Delta M$  between the magnetization before and after the pulse as a function of the pulse length  $w$ .  $\Delta M$  increases linearly with  $w$  for short pulses of few tens of ns. It saturates for  $w \approx 10 \mu$ s and decrease for very long pulses because of cryostat heating effects. Nonresonant photon absorption is also observed for very long pulses.

The resonant photon absorption lines are often taken to estimate a lower bound on the decoherence time of a qubit. We therefore investigated in more detail the line width observed in Fig. 2. Figure 4(a) presents a typical power dependence of the line width for continuous irradiation at 4.2 GHz. Resonant photon absorption is clearly visible for a generator power larger than  $-60$  dBm (1 nW). The line saturated at about  $-20$  dBm (10  $\mu$ W). Figure 4(b) presents the absorption line for the pulsed technique (see Fig. 2) for several pulse lengths and a generator power of 15 dBm (32 mW,  $B_{RF} \approx 1$  mT). The resonant photon absorption is clearly visible for pulse lengths longer than 10 ns. Note that the line widths for continuous irradiation at low power [Fig. 4(a)] are nearly twice as large as those for pulsed irradiation [Fig. 4(b)]. This suggests inhomogeneous broadening.

In order to shed light on the origin of the line width broadening, we developed a two-pulse hole-burning technique. The first pulse excites a fraction of spins that are in resonance during the pulse. In case of an inhomogeneous

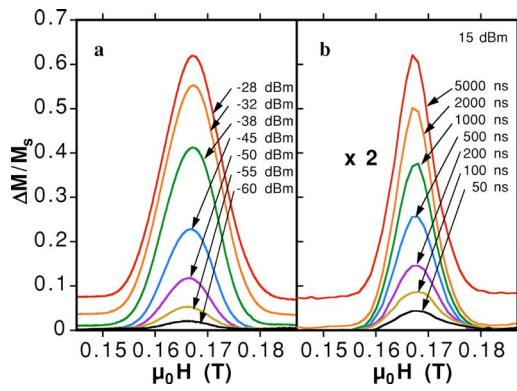


FIG. 4. (Color online) (a) Magnetization variation  $\Delta M$  between the equilibrium curves measured without and with continuous irradiation. The microwave frequency was 4.2 GHz. The microwave powers of the generator are indicated. (b) Magnetization variation  $\Delta M$  after a RF pulse of 4.2 GHz and several pulse lengths. The cryostat temperature was 40 mK.  $\Delta M$  is multiplied by a factor two.

broadened line, the first pulse burns a hole into the line. Then, after a delay time  $t_d$  a second pulse of the same frequency is applied. For  $t_d=0$  the two pulses are equivalent to one long pulse that excites a certain amount of spins (dotted lines in Fig. 5). However, for nonzero delay times  $t_d$  the second pulse probes the evolution of spin excitation in the sample. For an inhomogeneously broadened line, the second pulse probes whether the burnt hole of the first pulse evolved during the delay time. Figure 5 shows the resulting magnetization variation  $\Delta M$  after two pulses as a function of delay time. It is shown that for  $t_d > 100$  ns,  $\Delta M$  is clearly larger than for  $t_d=0$ . This result suggests that the absorption lines in Figs. 2 and 4 are inhomogeneously broadened (at these time scales). The first pulse burns a hole into the line which starts to fill during the delay time. The filling time is clearly faster for an applied field in the center of the line [Fig. 5(a)] than at the border [Fig. 5(b)]. It also depends on the pulse length: the longer the pulse length, the later the hole starts to fill. Because the magnetization is relaxing back to equilibrium at a much longer time scale (phonon bottleneck regime), the hole filling can only be due to spins that are close to the resonance condition. Due to spin-spin interactions, the excited spins can give their energy to those spins, that is the energy diffuses from the excited spins to spins that are close to the resonance condition. The hole filling time is therefore dominated by spin-spin interactions and it can be called an energy diffusion time.

In our case of an assembly of identical spins, the line broadening is mainly due to dipolar and hyperfine interactions. The dipolar coupling energy can be estimated with  $E_{\text{dip}}/k_B \approx (g\mu_B S)^2/V \approx 0.1$  mK ( $S=1/2$  and  $V=6.3$  nm<sup>3</sup>).<sup>6</sup> The hyperfine coupling with the nuclear spins can be obtained by considering the dipolar interaction of one Cr ion ( $s=3/2$ ) with the neighboring F nucleus having a nuclear spin  $I=1/2$ . With  $g_F=+5.26$  and the distance of  $d=0.2$  nm between F and Cr ions, the interaction energy is about 0.4 mK for each of the eight F nuclear spins.<sup>6</sup> The hyperfine line broadening of all eight F nuclear spins is about 3 mK

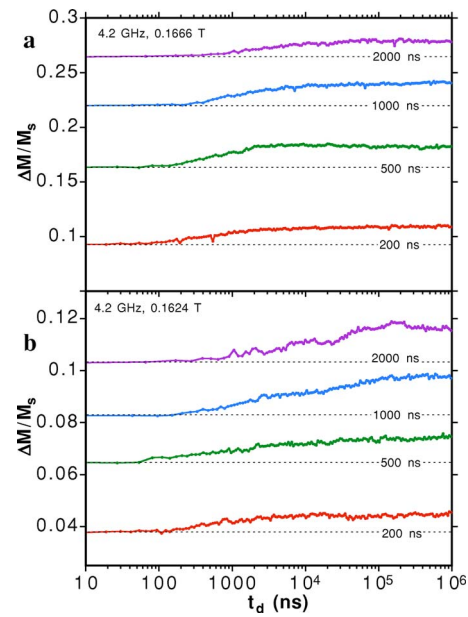


FIG. 5. (Color online) Magnetization variation  $\Delta M$  after two pulses of equal length as a function of delay time  $t_d$  between the pulses, (a) at an applied field of 0.1666 T corresponding to maximum resonance absorption, and (b) at 0.1624 T. The RF frequency is 4.2 GHz and the pulse lengths are indicated. The dotted lines indicate  $\Delta M$  for  $t_d=0$ .

which corresponds to 5 mT, in good agreement with the observed Gaussian line widths of about  $\sigma=4$  mT in Figs. 2 and 4.

Finally, we discuss the possibility of observing Rabi oscillations with the present set-up. Due to inhomogeneous broadening only a lower bound of the coherence time  $\tau_c$  can be estimated from the resonance lines in Fig. 4:  $\tau_c \approx B_p/(\sigma\nu) \approx 10$  ns with  $B_p=0.166$  T,  $\sigma=4$  mT, and  $\nu=4.2$  GHz. The corresponding number of coherent flips of the spin system is given by  $N=\tau_c/\tau_{\text{Rabi}}$  with  $\tau_{\text{Rabi}}=2\pi/(\gamma B_{\text{RF}}) \approx 40$  ns for  $B_{\text{RF}} \approx 1$  mT. We obtain  $N \approx 0.25$  showing that there is no hope to see Rabi oscillations in the present conditions. In order to get  $N \gg 1$ , it will be necessary to increase further the radiation field  $B_{\text{RF}}$ , to reduce substantially the hyperfine broadening by substituting the F ions with OH groups, and to minimize the dipolar coupling by doping the crystal of Cr<sub>7</sub>Ni molecules with Cr<sub>8</sub> molecules.

In conclusion, we presented magnetization measurements on a crystal of Cr<sub>7</sub>Ni antiferromagnetic rings. Irradiation with microwaves at frequencies between 1 and 10 GHz leads to observation of very narrow resonant photon absorption lines which are broadened by spin-spin interactions. A two-pulse hole-burning technique allowed us to estimate the characteristic energy diffusion time (spectral diffusion) giving an upper bound of  $T_1$  which is important to know for quantum computing problems.

This work was supported by the EC-TMR Network QuEMolNa (MRTN-CT-2003-504880), EPSRC(UK), INTAS, CNRS, and Rhône-Alpe funding.

- <sup>1</sup>D. Awschalom, N. Samarth, and D. Loss, *Semiconductor Spintronics and Quantum Computation* (Springer, Berlin, 2002).
- <sup>2</sup>M. N. Leuenberger and D. Loss, *Nature (London)* **410**, 789 (2001).
- <sup>3</sup>F. Meier, J. Levy, and D. Loss, *Phys. Rev. Lett.* **90**, 047901 (2003).
- <sup>4</sup>F. Meier, J. Levy, and D. Loss, *Phys. Rev. B* **68**, 134417 (2003).
- <sup>5</sup>F. Troiani, M. Affronte, S. Carretta, P. Santini, and G. Amoretti, *Phys. Rev. Lett.* **94**, 190501 (2005).
- <sup>6</sup>F. Troiani, A. Ghirri, M. Affronte, S. Carretta, P. Santini, G. Amoretti, S. Piligkos, G. Timco, and R. E. P. Winpenny, *Phys. Rev. Lett.* **94**, 207208 (2005).
- <sup>7</sup>J. Overgaard, B. B. Iversen, S. P. Palii, G. A. Timco, N. V. Gerbeleu, and F. K. Larsen, *Chem.-Eur. J.* **8**, 2775 (2002).
- <sup>8</sup>F. K. Larsen, E. J. L. McInnes, H. El Mkami, J. Overgaard, S. Piligkos, G. Rajaraman, E. Rentschler, A. A. Smith, G. M. Smith, V. Boote, M. Jennings, G. A. Timco, and R. E. P. Winpenny, *Angew. Chem., Int. Ed.* **42**, 101 (2003).
- <sup>9</sup>S. Carretta, P. Santini, G. Amoretti, M. Affronte, A. Ghirri, I. Sheikin, S. Piligkos, G. Timco, and R. E. P. Winpenny, *Phys. Rev. B* **72**, 060403 (2005).
- <sup>10</sup>W. Wernsdorfer, A. Müller, D. Maily, and B. Barbara, *Europhys. Lett.* **66**, 861 (2004).
- <sup>11</sup>L. Sorace, W. Wernsdorfer, C. Thirion, A.-L. Barra, M. Pachioni, D. Maily, and B. Barbara, *Phys. Rev. B* **68**, 220407(R) (2003).
- <sup>12</sup>E. del Barco, A. D. Kent, E. C. Yang, and D. N. Hendrickson, *Phys. Rev. Lett.* **93**, 157202 (2004).
- <sup>13</sup>M. Bal, J. R. Friedman, Y. Suzuki, K. M. Mertes, E. M. Rumberger, D. N. Hendrickson, Y. Myasoedov, H. Shtrikman, N. Avraham, and E. Zeldov, *Phys. Rev. B* **70**, 100408 (2004).
- <sup>14</sup>K. Petukhov, W. Wernsdorfer, A.-L. Barra, and V. Mosser, *Phys. Rev. B* **72**, 052401 (2005).
- <sup>15</sup>M. Bal, J. R. Friedman, Y. Suzuki, E. M. Rumberger, D. N. Hendrickson, N. Avraham, Y. Myasoedov, H. Shtrikman, and E. Zeldov, *Europhys. Lett.* **71**, 110 (2005).
- <sup>16</sup>B. Cage, S. E. Russek, *Rev. Sci. Instrum.* **75**, 4401 (2004); B. Cage, S. E. Russek, D. Zipse, and N. Dalal, *J. Appl. Phys.* **97**, 10M507 (2005).
- <sup>17</sup>G. A. Candela, *J. Chem. Phys.* **42**, 113 (1965).
- <sup>18</sup>W. Wernsdorfer, *Adv. Chem. Phys.* **118**, 99 (2001).
- <sup>19</sup>C. Thirion, W. Wernsdorfer, and D. Maily, *Nat. Mater.* **2**, 524 (2003).
- <sup>20</sup>I. Chiorescu, W. Wernsdorfer, A. Müller, H. Bögge, and B. Barbara, *Phys. Rev. Lett.* **84**, 3454 (2000).
- <sup>21</sup>A. Abragam and B. Bleaney, *Electron Paramagnetic Resonance of Transition Ions* (Clarendon, Oxford, 1970).